Regenerative Therapy 18 (2021) 182–190

Contents lists available at ScienceDirect

Regenerative Therapy

journal homepage: http://www.elsevier.com/locate/reth

Original Article

Adipose-derived mesenchymal stem cells preserve cardiac function via ANT-1 in dilated cardiomyopathy hamster model

Daisuke Mori [a], Shigeru Miyagawa [a], Takashi Kido [a], Hiroki Hata [a], Takayoshi Ueno [a], Koichi Toda [a], Toru Kuratani [a], Miwa Oota [b], Kotoe Kawai [b], Hayato Kurata [b], Hiroyuki Nishida [c], Yoshiki Sawa [a, c, *]

[a] Department of Cardiovascular Surgery, Osaka University Graduate School of Medicine, Suita, Japan
[b] Institute of Advanced Stem Cell Therapy, Osaka University, Osaka, Japan
[c] Medical Center for Translational Research, Osaka University Hospital, Osaka, Japan

ARTICLE INFO

Article history:
Received 14 April 2021
Received in revised form
2 June 2021
Accepted 21 June 2021

Keywords:
Mesenchymal stem cells
Idiopathic dilated cardiomyopathy
ATP
Mitochondrial transporter

ABSTRACT

Introduction: Idiopathic dilated cardiomyopathy (DCM) is associated with abnormalities in cytoskeletal proteins, mitochondrial ATP transporter, microvasculature, and fibrosis. Mesenchymal stem cells (MSCs) can ameliorate distressed mitochondrial and structural proteins, as well as fibrosis, via the paracrine effect of cytokines. This study aimed to investigate whether the transplantation of adipose tissue-derived MSCs (ADSCs) reverses histological and functional abnormalities in the distressed myocardium of DCM-like hamsters by modulating the expression of adenine nucleotide translocase 1 (ANT-1).
Methods: Eighteen weeks after birth, ADSCs were implanted onto the cardiac surface of δ-sarcoglycan (SG)-deficient hamsters or sham surgery was performed.
Results: Left ventricular ejection fraction and end-systolic diameter were maintained in ADSC-treated animals for four weeks, ATP concentration was considerably elevated in the cardiomyocytes of these animals, and ANT-1 expression was significantly upregulated as well. The expression of extracellular matrix and myocardial cytoskeletal proteins, such as collagen, SG, and α-dystroglycan, did not differ between groups. However, significant improvements in myosin and Smad4 expression, cardiomyocyte hypertrophy, and capillary density occurred in the ADSC-treated group.
Conclusions: We demonstrated that ADSCs might maintain cardiac function in the DCM hamster model by enhancing ATP concentration, as well as mitochondrial transporter and myosin expression, indicating their potential for DCM treatment.

1. Introduction

Idiopathic dilated cardiomyopathy (DCM) has been reported to result from several pathophysiological conditions, including abnormalities in cytoskeletal proteins, mitochondrial ATP transporters, microvasculature, and fibrosis, all of which may be primary therapeutic targets [1–3]. Cell therapy has been established to be useful for treating ischemic cardiomyopathy (ICM), where cardiomyocytes experience ischemia and hibernation along with ATP upregulation. However, neither the efficacy of cell therapy for DCM nor the mechanism responsible for ATP upregulation in DCM have been characterized [4].

Furthermore, the pathophysiology of DCM includes inflammation, microvasculopathy, free radical stress with mitochondrial dysfunction, apoptosis of cardiomyocytes, remodeling of the extracellular matrix, and homeostatic abnormality in collagen turnover [1,2]. In particular, abnormal expression of adenine nucleotide translocase 1 (ANT-1), an antiporter of ATP and ADP in

Abbreviations: ADSC, Adipose tissue-derived mesenchymal stem cells; ANOVA, Analyses of variance; EF, Ejection fraction; HGF, Human growth factor; LV, Left ventricle; OD, Optical density; SEM, Standard error of the mean; TGFR, Transforming growth factor receptor; VEGF, Vascular endothelial growth factor.

* Corresponding author. Department of Cardiovascular Surgery, Osaka University Graduate School of Medicine, 2-2 Yamadaoka, Suita, Osaka, 565-0871, Japan. Fax: +81-6-6879-3163.
E-mail address: sawa-p@surg1.med.osaka-u.ac.jp (Y. Sawa).

Peer review under responsibility of the Japanese Society for Regenerative Medicine.

https://doi.org/10.1016/j.reth.2021.06.006

the myocardial mitochondria, plays an essential role in the onset of DCM [2,5–7]. Therefore, methods for regulating and enhancing ANT-1 expression and ATP concentration in the cytoplasm may offer therapeutic options for idiopathic DCM.

Previous reports suggest that cell transplantation may be effective by targeting a different mechanism from those targeted by current drug therapies, making it a potential option to treat idiopathic DCM. Therefore, we sought to investigate whether the transplantation of adipose tissue-derived mesenchymal stem cells (ADSCs) reverses histological and functional abnormalities in the distressed myocardium of the idiopathic DCM hamster model via modulation of ANT-1 expression.

Herein, we examined ANT-1 activity in the myocardium of J2N-k hamsters exhibiting the DCM phenotype with concomitant reductions in ATP concentration and myocardial contraction [8,9]. The therapeutic potential of ADSCs was also evaluated in J2N-k hamsters. We also measured the expression of several cytokines, including transforming growth factor (TGF)-β, which may regulate ANT-1 expression [10], to further elucidate the potential associated mechanisms.

2. Methods

2.1. Human ADSC graft preparation

Healthy human ADSCs were purchased from Lonza (Basel, Switzerland) and cultured at 37 °C in the presence of 5% CO_2 for 2–3 days. Then, the ADSCs were subcultured four times and cryopreserved.

2.2. ADSC administration to DCM hamsters

Eighteen-week-old male δ-sarcoglycan-deficient J2N-k hamsters and J2N-n healthy hamsters (Japan SLC, Shizuoka, Japan) were used as idiopathic and wild models, respectively. J2N-k hamsters develop human DCM-like histopathological features associated with the deterioration of cardiac function [2]. All hamsters underwent left lateral thoracotomy under 1.5% isoflurane anesthesia. Subsequently, ADSCs were delivered into the heart using a novel method, in which a fibrinogen and thrombin solution containing ADSCs was pipetted and dropped on the surface of the heart, covering the entire left ventricular surface (1×10^6 cell/body) (Group ADSC, $n = 10$) (S1 Table) [11]. The hamsters in the other groups—J2N-n wild hamsters (Group Wild, $n = 10$) or sham surgery for J2N-k hamsters (Group Sham, $n = 10$)—underwent ADSC-free fibrinogen/thrombin solution treatment in the same manner as Group ADSC. After transplantation, the hamsters were housed in temperature-controlled individual cages until natural death occurred or were euthanized using excessive anesthesia (4% isoflurane) followed by exsanguination and removal of the heart at two or four weeks post-surgery ($n = 5$ each) (Fig. 1).

2.3. Evaluation of cardiac function with transthoracic echocardiography

Transthoracic echocardiography was performed using a system equipped with a 12-MHz transducer and Vivid-i (GE Healthcare, Chicago, IL, USA) under isoflurane inhalation (1%). Diastolic/systolic dimensions (Dd/Ds) and ejection fraction (EF) of the left ventricle (LV) were measured.

2.4. Isolation of mitochondria from the heart

The mitochondrial fractions from heart tissue samples were isolated using a mitochondria isolation kit (CosmoBio, Tokyo, Japan) following the manufacturer's protocol. Briefly, cardiac tissues, which were harvested, snap-frozen, and stored at −80 °C, were immersed in ice-cold buffer A and homogenized on ice. The homogenate was applied onto a filter cartridge and centrifuged at 16,000×*g* for 30 s to remove the cells and large debris. Next, the filtered supernatant was added to buffer B and centrifuged at 16,000×*g* for 10 min; the supernatant obtained was discarded. The pellet was resuspended in buffer B and centrifuged at 8000×*g* for 5 min. Ice-cold phosphate-buffered saline solution was added to the collected supernatant and centrifuged at 16,000×*g* for 15 min. The final pellet contained the mitochondria.

2.5. ATP quantification in the heart

ATP content was assessed using a colorimetric ATP assay kit (Abcam, Cambridge, UK). Frozen heart samples were homogenized and centrifuged at 15,000×*g* for 2 min, and the ATP content in the resultant supernatant was assessed. The standard curve for ATP and the reaction mixture were prepared according to the manufacturer's instructions in a 96-well plate, and optical density was measured at 570 nm using the Infinite F200 PRO microplate reader (Tecan, Männedorf, Switzerland).

2.6. Protein expression in the heart

Protein concentrations were determined using the Pierce BCA protein assay kit (Thermo Fisher Scientific, Waltham, MA, USA) according to the manufacturer's instructions. Whole mitochondrial pellets were solubilized in Laemmli buffer and 10 μg of proteins was separated by using electrophoresis on a 10% sodium dodecyl sulfate (SDS)-polyacrylamide gradient gel and transferred onto a polyvinylidene fluoride (PVDF) membrane. Nonspecific binding was blocked with StartingBloc blocking buffer (Thermo Fisher Scientific) and the membranes were incubated with specific antibodies. The antibodies used were anti-ANT-1 (1:500, ab102032) and anti-cytochrome c oxidase (COX IV; 1:1,000, ab16056) and were purchased from Abcam. Afterwards, the membranes were incubated with anti-rabbit IgG-horse radish peroxidase (HRP)-linked secondary antibodies. After developing the membranes using an enhanced chemiluminescence kit (CosmoBio), the signals were visualized using the ChemiDoc XRS+ system (BioRad, Hercules, CA, USA). Cytochrome c oxidase expression was used as internal control. The values obtained were expressed as a percentage of the value in the J2N-n hamsters (ImageLab Ver 6.0, BioRad).

2.7. Cytokine secretion from the ADSC graft

Human ADSCs after the 4th passage were used to form the small-scale graft in a 6-well plate using the method mentioned above and cultured for 72 h. The culture supernatant was collected, and the concentrations of various cytokines were assessed using an enzyme-linked immunosorbent assay kit (Quantikine ELISA, R&D Systems, Minneapolis, MN, USA).

2.8. Gene expression in the heart

Total RNA was isolated from the free wall of the LV using the RNeasy kit and reverse-transcribed using Omniscript reverse transcriptase (Qiagen, Hilden, Germany). Complementary DNA samples were prepared and assayed in duplicates. Quantitative polymerase chain reaction (qPCR) was performed with the ABI 7500 Fast real-time PCR system using SYBR Green real-time PCR master mix (Thermo Fisher Scientific) and specific primers/probes (S2 Table). The average copy number of the transcripts was

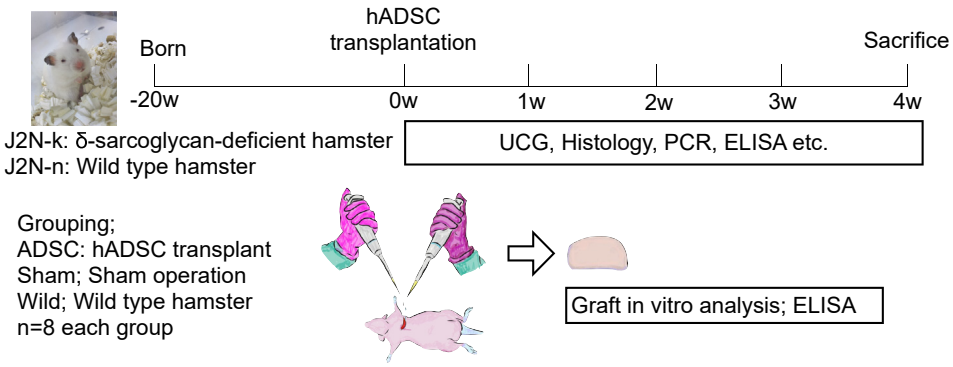

Fig. 1. Study protocol. Human ADSC grafts were implanted on the cardiac surface of 20-week-old J2N-k and -n hamsters.

normalized to that of glyceraldehyde-3-phosphate dehydrogenase (*Gapdh*) for each sample.

2.9. Histological analysis

Two or four weeks after transplantation, the heart was excised after euthanization with 5% isoflurane to perform histological analysis. The excised heart specimen was fixed with either 10% buffered formalin for paraffin sections or 4% paraformaldehyde for frozen sections. The paraffin sections were stained with hematoxylin-eosin and periodic acid–Schiff staining of the LV and picrosirius red to assess the degree of myocyte diameter and myocardial fibrosis. The paraffin sections were also immunohistologically labeled using anti-von Willebrand factor antibody, polyclonal anti-CD31 antibody (Abcam), anti-α-sarcoglycan (Novocastra Laboratories, Newcastle, UK), anti-β-sarcoglycan (Novocastra), and anti-α-dystroglycan (clone IIH6C4, Merck, Kenilworth, NJ, USA) to assess the capillary vascular density and the organization of cytoskeletal proteins. In addition, the TGF-β receptor and myosin in the myocardium were stained with anti-TGF-β receptor I antibody (Abcam) and anti-myosin light chain 2 antibody (Abcam), respectively.

The percentage of the total area that was fibrotic, as determined by picrosirius red staining, was calculated using a planimetric method with the MetaMorph software (Molecular Device, San Jose, CA, USA). The number of capillaries per square millimeter was calculated using the BZ Analyzer (Keyence, Osaka, Japan) and was counted in five high-

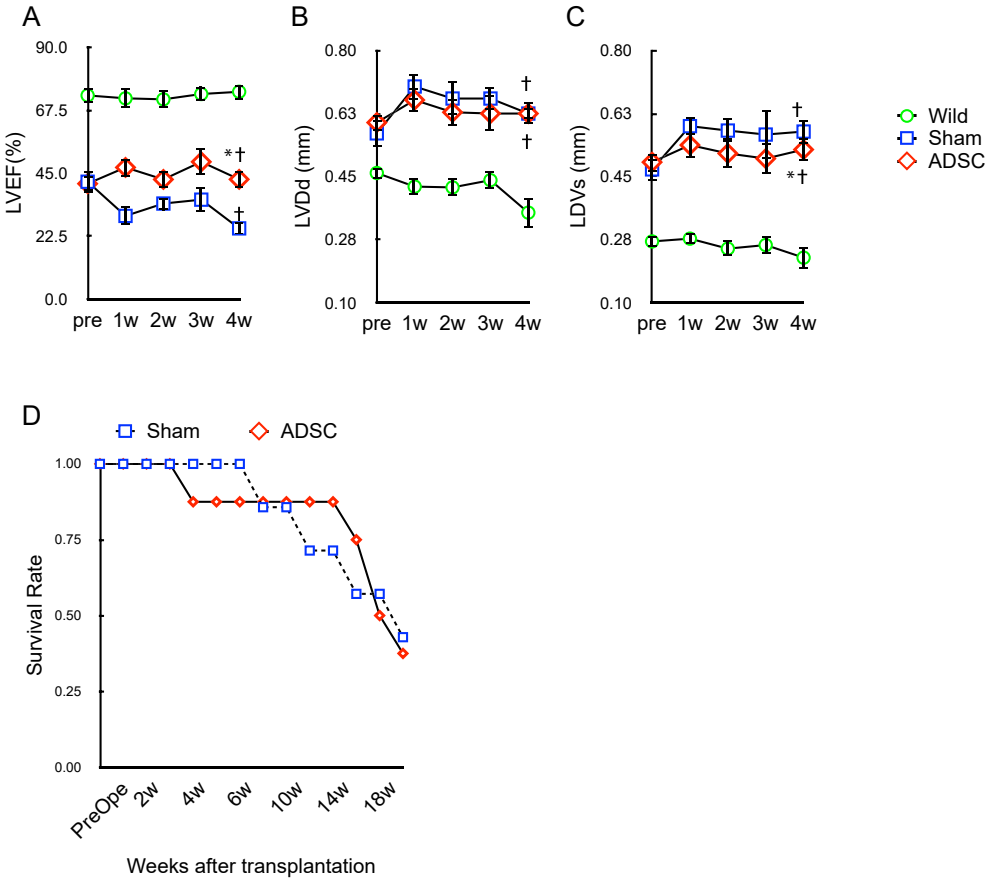

Fig. 2. Cardiac function and survival rate. (A–C) Echocardiographic evaluation of cardiac function after ADSC implantation. Kruskal–Wallis test was used to evaluate significant differences, with $*P < 0.05$ versus Group Sham and $\dagger P < 0.05$ versus Group Wild. (D) Overall survival rates after treatment were evaluated using the log-rank test. Groups Wild ($n = 8$), ADSC ($n = 8$), and Sham ($n = 7$).

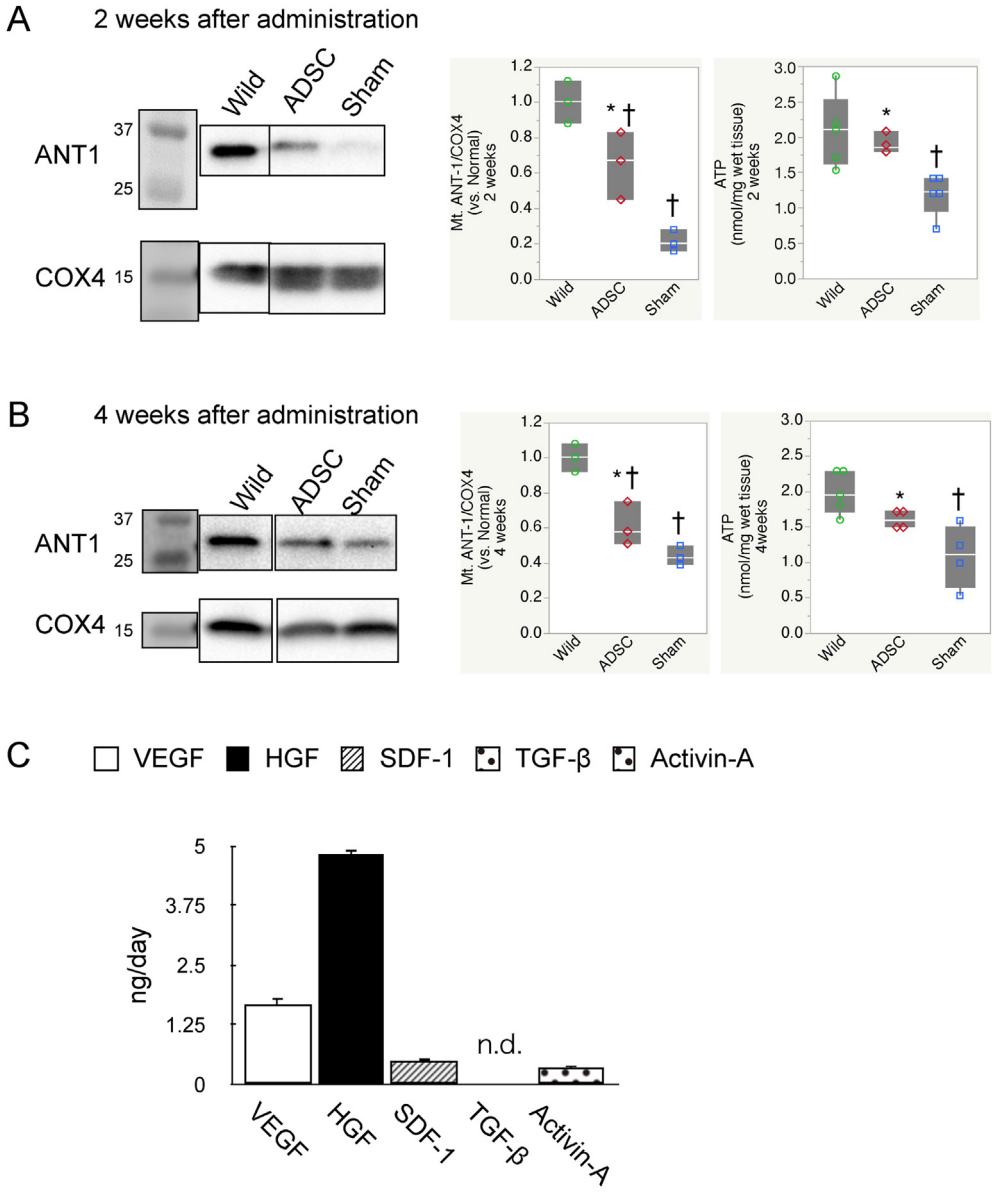

Fig. 3. ADSC graft characteristics. (A, B) Western blotting of mitochondrial ANT-1 and cytosolic ATP concentration in Groups ADSC and Sham at two and four weeks after ADSC transplantation. The blotting figure was cropped for clarity and full-length blots are presented in S1 Fig. (C) Cytokine secretion from ADSC graft. ANOVA and Student's *t*-test were used to evaluate significant differences, with **P* < 0.05 versus Group Sham and †*P* < 0.05 versus Group Wild.

power magnification fields per section (25 fields/heart) [12]. The percentage of the total area positive for α-sarcoglycan, β-sarcoglycan, and α-dystroglycan, as determined by immunohistochemical staining, was calculated using the BZ Analyzer.

2.10. Statistical analysis

Values are shown as the mean ± standard error of the mean. Student's *t*-test (two-tailed) was used to compare two groups of independent samples. One-way and two-way analyses of variance (ANOVA) with Bonferroni correction for multiple comparisons were performed to assess within- and between-group differences following the treatments. Following ANOVA, between-group comparisons were made using a Student's *t*-test (two-tailed). Survival curves were prepared using the Kaplan–Meier method and compared using the log-rank test. All probability values were two-sided. The JMP 13 software (SAS Institute, Cary, NC, USA) was used for all analyses. *P*-values <0.05 indicated statistical significance.

2.11. Ethics approval

All experimental procedures were approved by the Osaka University Institutional Ethics Committee (approval number 27-046-011). Animal care was in compliance with the Principles of Laboratory Animal Care formulated by the National Society for Medical Research and the Guide for the Care and Use of Laboratory Animals prepared by the Institute of Animal Resources and published by the National Institutes of Health (8th Edition, revised in 2011). All experimental animals were euthanized using sufficient analgesics to minimize animal suffering. To maximize reproducibility and potential for re-use of data, we followed the Animal Research: Reporting of *In Vivo* Experiments (ARRIVE) guidelines for all submissions describing laboratory-based animal research.

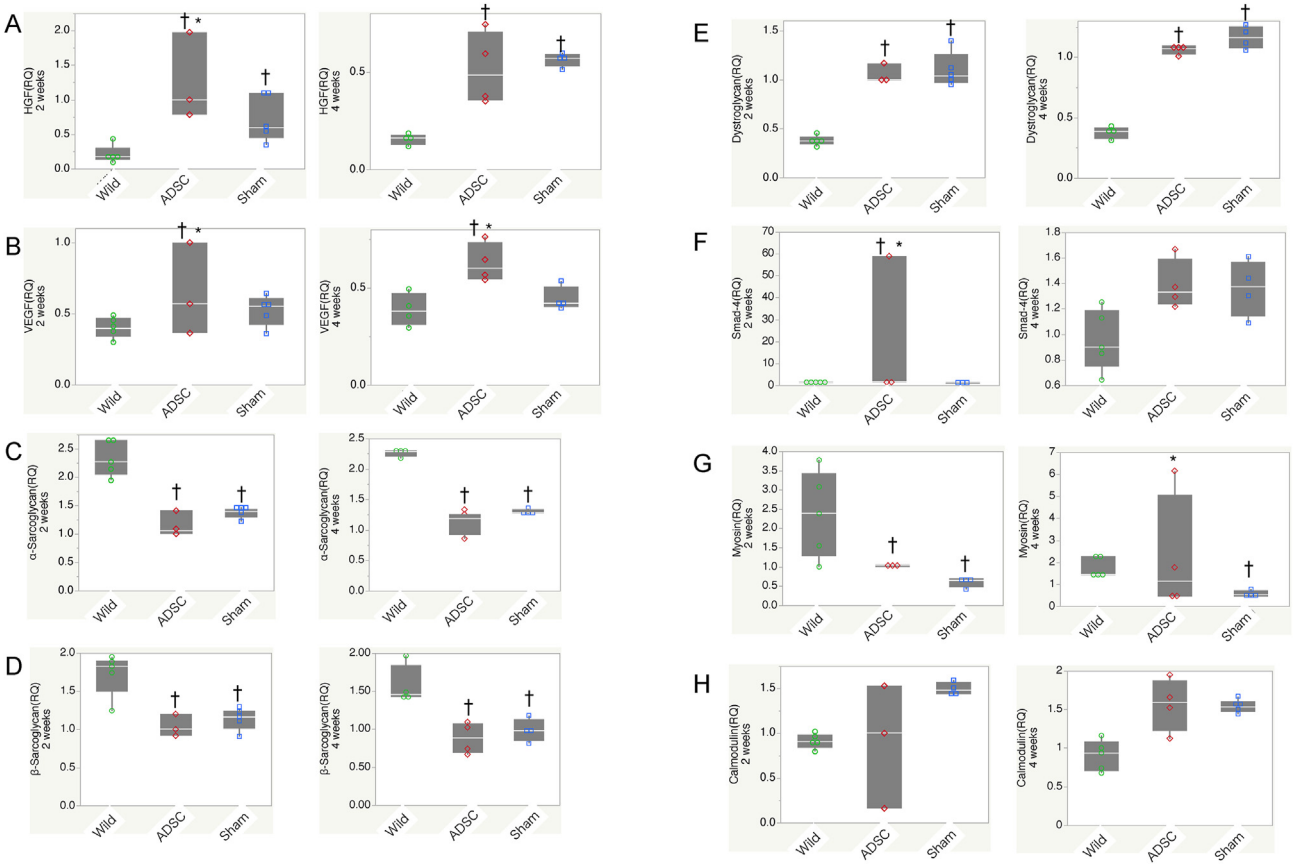

Fig. 4. Comparison of myocardial gene expression. The expression levels of α-sarcoglycan, β-sarcoglycan, and α-dystroglycan genes were evaluated in Groups ADSC and Sham at two and four weeks after transplantation. ANOVA and Student's *t*-test were used to identify significant differences, with $*P < 0.05$ versus Group Sham and $\dagger P < 0.05$ versus Group Wild.

3. Results

3.1. Cardiac performance and survival of DCM hamsters after ADSCs transplantation

The effects of ADSC transplantation on the cardiac function were assessed by echocardiography (Fig. 1). All DCM hamsters showed similar EF and LV Dd/Ds at 20 weeks before transplantation or sham operation. After transplantation, LVEF and LV Ds were preserved for four weeks in Group ADSC as opposed to Group Sham which showed progressive deterioration in LV Dd/Ds and LVEF. However, Group ADSC also exhibited a progressive worsening in LVEF and LV Dd/Ds in the subsequent weeks after the first four weeks (Fig. 2A–C). Furthermore, morbidity or mortality related to the surgery were not observed in either group, and the survival rates of hamsters in Groups ADSC and Sham showed similar overall disease progression over 18 weeks after intervention. However, the survival rate in the Group ADSC was slightly better at six weeks compared with the Group Sham, and the cause of death was believed to be congestive heart failure (Fig. 2D).

3.2. Intracellular ATP concentration and mitochondrial ANT-1 expression

Transplantation of ADSCs increased the expression of ANT-1 in the mitochondrial fraction of cardiomyocytes two weeks after implantation. At two and four weeks after transplantation, the cytosolic ATP concentration increased in the Group ADSC by 120% compared with the Group Sham (Fig. 3A and B, and S1 Fig.).

3.3. Cytokine secretion from ADSC graft in vitro

Conditioned media from the ADSC grafts contained various factors, such as human growth factor (HGF), vascular endothelial growth factor (VEGF), stromal cell-derived factor (SDF)-1, and activin-A, which have been previously reported to be cardioprotective and remodeling-suppressive factors. TGF-β1 and -β2 were not detected in the conditioned media after 72 h (Fig. 3C).

3.4. Regulation of signaling proteins and cytokines in the heart

The expression of signaling proteins and cytokine mRNAs in the hearts of animals from both cardiomyopathy model groups and of wild-type hamsters ($n = 3$ each) was then investigated. The expression of myocardial α-sarcoglycan (RQ), β-sarcoglycan (RQ), and dystroglycan (RQ) mRNA in Group ADSC did not differ from those in Group Sham at two and four weeks. In contrast, at two weeks, HGF, VEGF, and Smad4 were upregulated compared with Group Sham, whereas VEGF and myosin were also upregulated in Group ADSC at four weeks (Fig. 4).

3.5. Effect of ADSCs on myocardial fibrosis and heart vasculature

CD31-labeled sections of the heart of Groups ADSC and Sham, as well as from healthy wild hamsters, were assessed to identify the

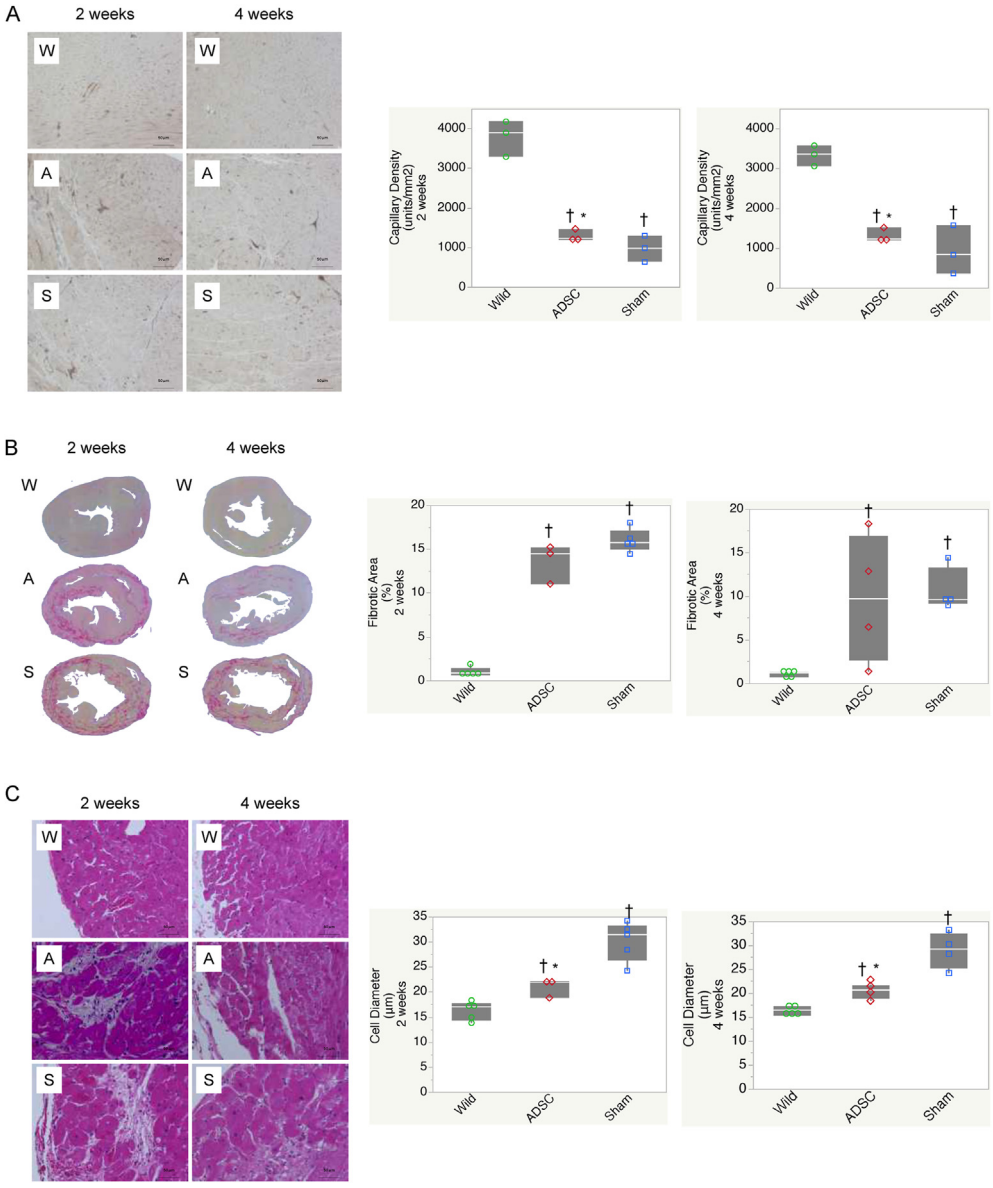

Fig. 5. Histological analysis of heart sections. (A) Capillary density was determined using anti-von Willebrand factor antibody, 14 and 28 days after ADSC implantation. (B) Quantification of the fibrotic area and representative picosirius red staining of whole heart section in each group, 14 and 28 days after ADSC implantation (C) Representative hematoxylin-eosin and periodic acid–Schiff staining of the LV. Cardiomyocyte diameter was measured in Groups ADSC and Sham. Kruskal–Wallis test revealed *$P < 0.05$ versus Group Sham and †$P < 0.05$ versus Group Wild.

trend in the distribution and number of arterioles and capillaries in the heart ($n = 5$, each). Fewer CD31-positive arterioles and capillaries were found in cardiac tissue samples from Group Sham than in healthy heart, at two and four weeks. In contrast, the number of arterioles and capillaries was higher in Group ADSC at two and four weeks compared with Group Sham (Fig. 5A). The distribution and quantity of interstitial collagen in the heart after implantation was assessed by picrosirius red staining ($n = 5$, each). As opposed to healthy hamsters, interstitial collagen accumulated in the J2N-k hamsters, irrespective of the treatment (Fig. 5B).

3.6. Organization of cytoskeletal proteins

The diameters of the cardiomyocytes were significantly smaller in Group ADSC (Fig. 5C). The trend in the expression of α-sarcoglycan, β-sarcoglycan, and α-dystroglycan in the hearts after ADSC treatment was comprehensively assessed using immunohistological analysis and qPCR. These three cytoskeletal proteins were found to be homogeneously expressed around the cardiomyocytes of healthy hamsters; however, they were scarcely expressed in the hearts of Group ADSC or Group Sham (Fig. 6A–C). In contrast, α-dystroglycan expression was higher in Group ADSC than in Group Sham at two and four weeks (Fig. 4C and D). Furthermore, the trend in myosin gene expression after ADSC transplantation was to be higher in Group ADSC compared with Group Sham. Although there were no apparent histological differences, myosin expression was upregulated in Group ADSC compared with Groups Wild and Sham four weeks after the treatment (Figs. 4G and 6D).

4. Discussion

In this study, we aimed to investigate whether epicardial transplantation of ADSCs reverses histological and functional abnormalities in the distressed myocardium of DCM hamster models via

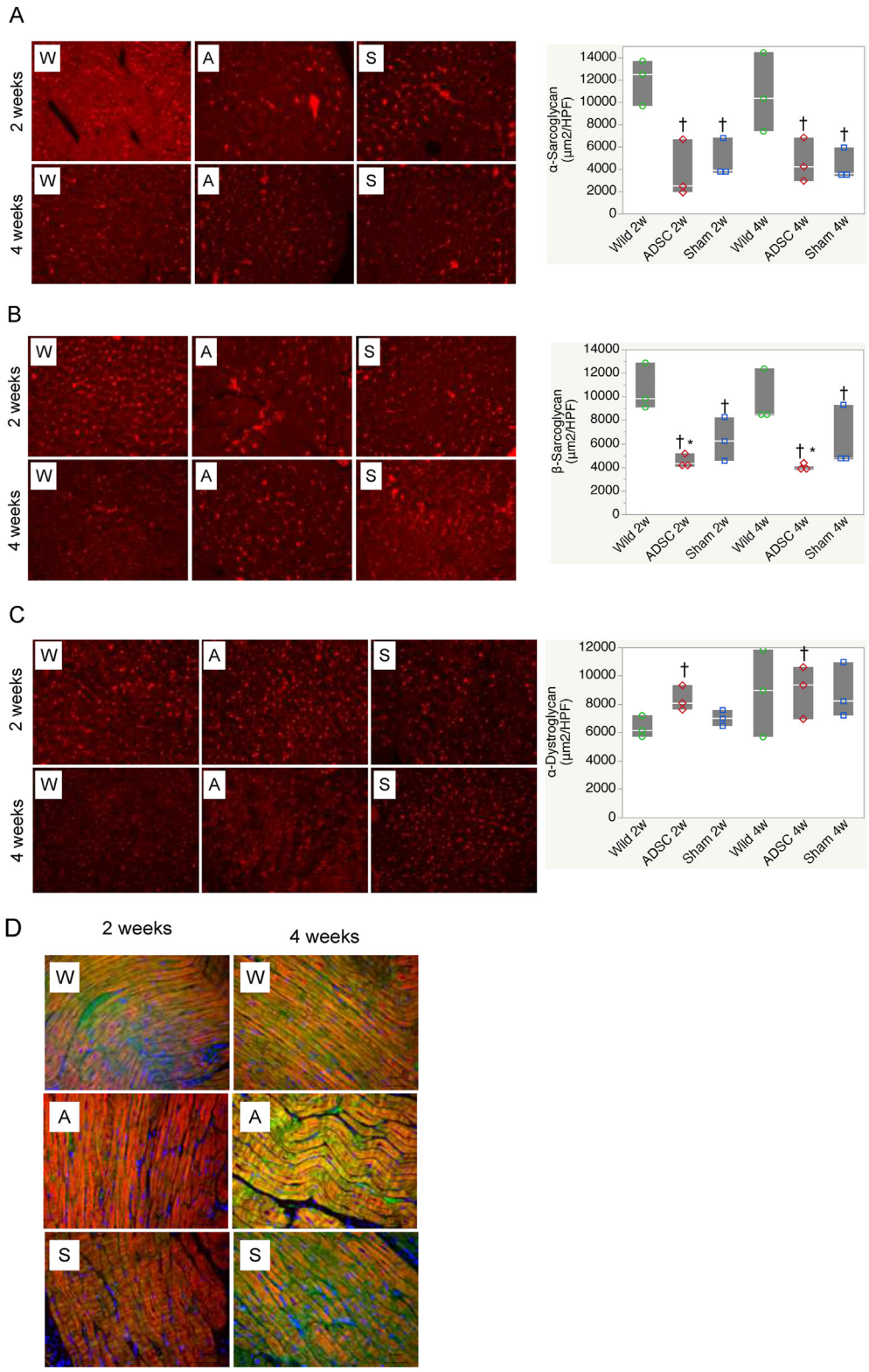

Fig. 6. Representative picture of ECM-stained left ventricular wall. (A, B) The α- and β-sarcoglycan levels were quantified in each group. (C) The α-dystroglycan level was also quantified in each group. ANOVA and Student's *t*-test were used to identify significant differences, with $*P < 0.05$ versus Group Sham and $\dagger P < 0.05$ versus Group Wild. (D) Representative picture of the myosin-stained left ventricular wall, two and four weeks after ADSC transplantation.

modulation of ANT-1 expression. Our results showed that although cardiac function gradually deteriorated within its natural course, cardiac output was maintained following ADSC transplantation in DCM-like hamsters, and this results were considered clinically meaningful in the sense that the transplantation method is simpler than other method [11]. The ATP concentration in the cytoplasm increased with ANT-1 upregulation. The activin-A secreted by ADSCs may act on the TGF-β receptor of cardiomyocytes to reinforce ANT-1

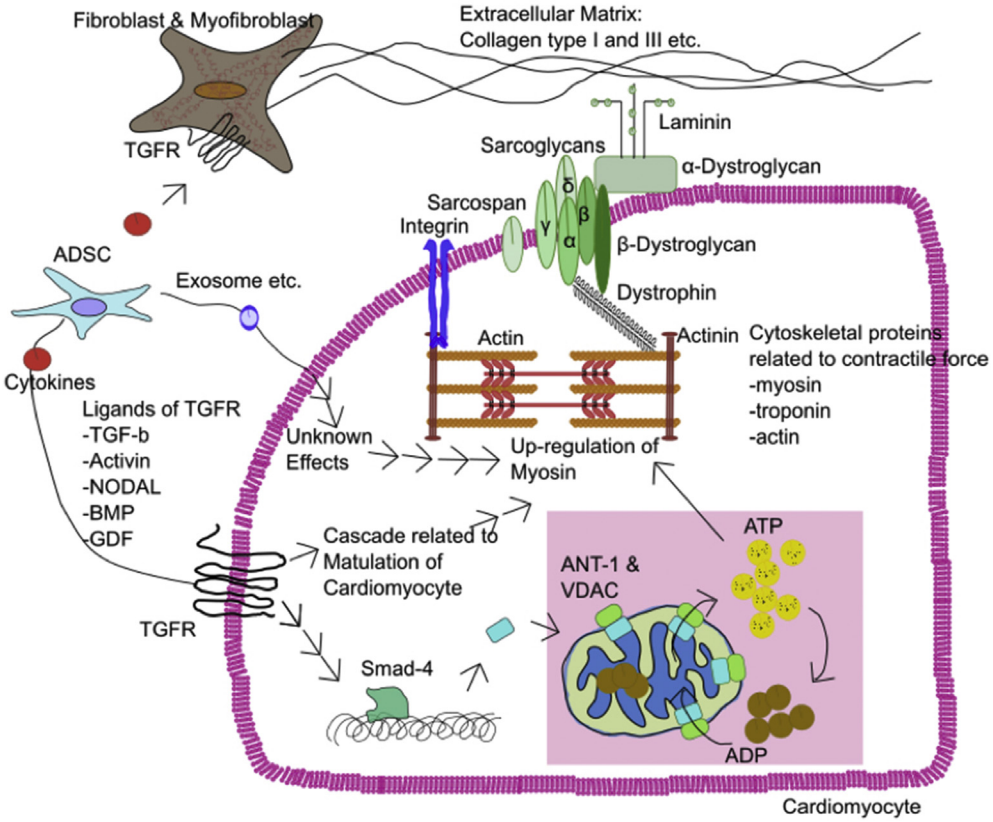

Fig. 7. Summary of the mechanism underlying ADSC therapy for dilated cardiomyopathy (DCM). The myocardial cascade via transforming growth factor receptor (TGFR) possibly enhances the expression of ANT-1 and myosin, which maintains myocardial contractility. In contrast, activin, a ligand of TGFR, is secreted from ADSCs. The possibility of activating fibroblasts was also considered.

expression via Smad4 activation. Based on these results, we hypothesized that this signal increased the expression of ANT-1, ATP production, and myosin expression, subsequently improving the cardiac contractile force [13]. Histologically, suppression of cardiomyocyte hypertrophy and vascularization were observed, in agreement with previous reports. However, suppression of myocardial fibrosis was not apparent in this study. Despite the levels of cytoskeletal proteins, including sarcoglycan and dystroglycan, remaining unaltered, myosin was upregulated (Fig. 7).

At the molecular level, the causes of heart failure are diverse and complex. The expression of myosin and other contraction-related proteins decreases in ischemic cardiomyopathy and idiopathic cardiomyopathy [14]. In this study, enhanced myosin expression and ATP production promoted contraction. Although the details of the underlying intracellular signals were not identified, it is important to note that myosin expression was restored with the enhancement of ANT-1 and ATP levels. The correlation between myocardial contractile force and the structural units of myosin has been studied, and a decrease in the expression or mutations in myosin and mitochondrial gene have been shown to directly cause cardiac dysfunction [13,15].

Previous studies have also shown that thyroid hormones function as humoral factors in regulating myosin expression. Furthermore, in addition to their primary effects, β-blockers used in patients with heart failure suppress myosin expression [16]. Although the myocardial intracellular signaling pathway starting from TGF-β is reportedly involved in the maturation of myocardial progenitor cells, a direct relationship with myosin expression was also demonstrated [17].

Fibrosis of myocardial tissue is an important prognostic factor not only in ischemic cardiomyopathy but also in dilated cardiomyopathy [17]. Other than cardiomyocytes, cardiac tissue also contains vascular endothelial cells, vascular smooth muscle cells, and myofibroblasts. TGF-β promotes myocardial fibrosis, primarily because of its effects on myofibroblasts and fibroblasts. Production of collagen type I, a typical extracellular matrix in cardiac remodeling, is promoted as fibroblasts are treated with TGF-β [10]. In addition, the involvement of immune cells in this cardiac remodeling has been reported, and it is thought that the control of immune cells is important only for the suppression of fibrosis [18].

Although several intracellular cascades have been reported to activate collagen production, the primary pathway involves TGF-β signaling, which activates the expression of Smads [10]. In this study, the ADSCs did not secrete TGF-β, but secreted activin, a partial agonist of the TGF-β receptor. As activin can act on both cardiomyocytes and fibroblasts, ANT-1 and ATP levels were possibly enhanced in cardiomyocytes, while fibroblasts promoted ECM production [16,19,20]. Although the cardiac function was clinically maintained, enhanced ANT-1 and ATP levels may not prevent cardiac remodeling or improve DCM prognosis statistically.

5. Conclusion

In conclusion, our results show that transplanting ADSCs onto the cardiac surface ameliorates the pathophysiology of DCM in the hamster model. Our data also demonstrated that ADSCs mediate an increase in ATP concentration in the cardiomyocytes by promoting ANT-1 expression, probably through the activin–TGF-β–Smad axis. As the heart comprises heterogeneous cells, interpretation of the mechanism of cytokine action, which exerts antagonistic effects on cardiac function as observed in this study, is difficult. Although

gene expression of the entire cardiac tissue was quantified, the expression patterns of a single cell type were not analyzed, which is a limitation of this study. In the future, the detailed mechanism underlying ADSC-based therapy should be analyzed using a single cell analysis approach after isolating different cell types from heart samples. Nevertheless, ADSC transplantation could be developed as a therapeutic option for DCM.

Authors' contributions

Conceptualization, D.M., S.M., and Y.S.; Investigation, D.M., M.O, K.K., H.K., and H.N.; Formal Analysis. M.O, K.K., H.K., and H.N.; Writing – Original Draft, D.M., S.M., and Y.S.; Writing – Review & Editing, D.M., S.M., H.H., T.U., K.T., T.K., and Y.S.

Ethics approval

All experimental procedures were approved by the Osaka University Institutional Ethics Committee (approval number 27-046-011).

Statement of human and animal rights

Animal care was in compliance with the Principles of Laboratory Animal Care formulated by the National Society for Medical Research and the Guide for the Care and Use of Laboratory Animals prepared by the Institute of Animal Resources and published by the National Institutes of Health (8th Edition, revised in 2011). All experimental animals were euthanized using sufficient analgesics to minimize animal suffering. To maximize reproducibility and potential for re-use of data, we followed the Animal Research: Reporting of *In Vivo* Experiments (ARRIVE) guidelines for all submissions describing laboratory-based animal research.

Statement of informed consent

No human subjects were used in this study and informed consent is not applicable.

Funding

This study was supported by Rohto Pharmaceutical Co., Ltd.

Declaration of competing interest

Dr. Sawa serves as an advisor for the sponsor (Rohto Pharmaceutical Co., Ltd.). Dr. Sawa and Dr. Miyagawa received a speaking fee from the sponsor. Ms. Oota, Ms. Kawai, Mr. Kurata, and Mr. Nishida receive salaries from the sponsor where they are employees. The sponsor had no control over the interpretation, writing, or publication of this work. The terms of this arrangement have been reviewed and approved by Osaka University in accordance with its policy on objectivity in research.

Acknowledgments

The authors thank Akima Harada for providing excellent technical assistance.

Appendix A. Supplementary data

Supplementary data to this article can be found online at https://doi.org/10.1016/j.reth.2021.06.006.

References

[1] Kim HK, Nilius B, Kim N, Ko KS, Rhee BD, Han J. Cardiac response to oxidative stress induced by mitochondrial dysfunction. Rev Physiol Biochem Pharmacol 2016;170:101–27.
[2] Narula N, Zaragoza MV, Sengupta PP, Li P, Haider N, Verjans J, et al. Adenine nucleotide translocase 1 deficiency results in dilated cardiomyopathy with defects in myocardial mechanics, histopathological alterations, and activation of apoptosis. JACC Cardiovasc Imaging 2011;4:1–10.
[3] Weintraub RG, Semsarian C, Macdonald P. Dilated cardiomyopathy. Lancet 2017;390:400–14.
[4] Wen Y, Ding J, Zhang B, Gao Q. Bone marrow-derived mononuclear cell therapy for nonischaemic dilated cardiomyopathy-A meta-analysis. Eur J Clin Invest 2018;48:e12894.
[5] Dörner A, Schulze K, Rauch U, Schultheiss HP. Adenine nucleotide translocator in dilated cardiomyopathy: pathophysiological alterations in expression and function. Mol Cell Biochem 1997;174:261–9.
[6] Palmieri L, Alberio S, Pisano I, Lodi T, Meznaric-Petrusa M, Zidar J, et al. Complete loss-of-function of the heart/muscle-specific adenine nucleotide translocator is associated with mitochondrial myopathy and cardiomyopathy. Hum Mol Genet 2005;14:3079–88.
[7] Dörner A, Schultheiss HP. The myocardial expression of the adenine nucleotide translocator isoforms is specifically altered in dilated cardiomyopathy. Herz 2000;25:176–80.
[8] Kato M, Yang J, Iwai T, Tanamura A, Arino T, Kawashima O, et al. Abnormalities of ADP/ATP carrier protein in J-2-N cardiomyopathic hamsters. Mol Cell Biochem 1993;119:89–94.
[9] Dörner A, Schultheiss HP. Adenine nucleotide translocase in the focus of cardiovascular diseases. Trends Cardiovasc Med 2007;17:284–90.
[10] Dobaczewski M, Chen W, Frangogiannis NG. Transforming growth factor (TGF)-β signaling in cardiac remodeling. J Mol Cell Cardiol 2011;51:600–6.
[11] Mori D, Miyagawa S, Yajima S, Saito S, Fukushima S, Ueno T, et al. Cell spray transplantation of adipose-derived mesenchymal stem cell recovers ischemic cardiomyopathy in a porcine model. Transplantation 2018;102:2012–24.
[12] Linard C, Brachet M, L'homme B, Strup-Perrot C, Busson E, Bonneau M, et al. Long-term effectiveness of local BM-MSCs for skeletal muscle regeneration: a proof of concept obtained on a pig model of severe radiation burn. Stem Cell Res Ther 2018;9:299.
[13] Li J, King NC, Sinoway LI. ATP concentrations and muscle tension increase linearly with muscle contraction. J Appl Physiol (1985) 2003;95:577–83.
[14] Kung GL, Vaseghi M, Gahm JK, Shevtsov J, Garfinkel A, Shivkumar K, et al. Microstructural infarct border zone remodeling in the post-infarct swine heart measured by diffusion tensor MRI. Front Physiol 2018;9:826.
[15] Ramaccini D, Montoya-Uribe V, Aan FJ, Modesti L, Potes Y, Matter ML. Mitochondrial function and dysfunction in dilated cardiomyopathy. Front Cell Dev Biol 2020;8:624216.
[16] Nishi H, Ono K, Horie T, Nagao K, Kinoshita M, Kuwabara Y, et al. MicroRNA-27a regulates beta cardiac myosin heavy chain gene expression by targeting thyroid hormone receptor beta1 in neonatal rat ventricular myocytes. Mol Cell Biol 2011;31:744–55.
[17] Jung H, Kim HH, Lee DH, Hwang YS, Yang HC, Park JC. Transforming growth factor-beta 1 in adipose derived stem cells conditioned medium is a dominant paracrine mediator determines hyaluronic acid and collagen expression profile. Cytotechnology 2011;63:57–66.
[18] Daisuke M, Shigeru M, Ryohei M, Nagako S, Satsuki F, Takayoshi U, et al. Pioglitazone strengthen therapeutic effect of adipose-derived regenerative cells against ischemic cardiomyopathy through enhanced expression of adiponectin and modulation of macrophage phenotype. Cardiovasc Diabetol 2019;18:39.
[19] Ishimaru K, Miyagawa S, Fukushima S, Saito A, Sakai Y, Ueno T, et al. Synthetic prostacyclin agonist, ONO1301, enhances endogenous myocardial repair in a hamster model of dilated cardiomyopathy: a promising regenerative therapy for the failing heart. J Thorac Cardiovasc Surg 2013;146:1516–25.
[20] Park SE, Lee J, Chang EH, Kim JH, Sung JH, Na DL, et al. Activin A secreted by human mesenchymal stem cells induces neuronal development and neurite outgrowth in an in vitro model of Alzheimer's disease: neurogenesis induced by MSCs via activin A. Arch Pharm Res 2016;39:1171–9.